

INTERNATIONAL JOURNAL OF CHEMICAL REACTOR ENGINEERING

Volume 8

2010

Article A8

Modeling and Simulation of Industrial Continuous Naphtha Catalytic Reformer Accompanied with Delumping the Naphtha Feed

Mohammad Mahdavian*

Shohreh Fatemi[†]

Ali Fazeli[‡]

*University of Tehran, mahdavian@gmail.com

[†]University of Tehran, shfatemi@ut.ac.ir

[‡]University of Tehran, alifazeli@ut.ac.ir

Modeling and Simulation of Industrial Continuous Naphtha Catalytic Reformer Accompanied with Delumping the Naphtha Feed*

Mohammad Mahdavian, Shohreh Fatemi, and Ali Fazeli

Abstract

Nowadays, with the worldwide, increasing demands of the high qualitative gasoline, it is necessary to establish new naphtha reforming units and develop the traditional units to the high efficiency processes. In this work, according to the recent progresses in naphtha reforming technology, a mathematical modeling of a continuous catalytic reformer with catalyst recirculation is developed for simulation and optimization of the new industrial continuous reformers. The process model uses an extended version of the kinetic model reported by Padmavathi, with some modifications on kinetic constants, and it considers the deactivation rate of the catalyst and pressure drop within the reactor. The process model is based on a 12-lumped kinetics reaction network and has been proved to be quite effective in terms of an industrial application. The naphtha is based on 25-lumped pseudo-components (including C_6 to C_{10} hydrocarbons) in three categories of n-paraffins, isoparaffins, naphthens, including cyclopentanes and cyclohexanes, and aromatics. The light hydrocarbons product, consisting of C_1 to C_5 n-paraffins, is taken into account as the products of hydrocracking reaction. First, the kinetic parameters of the reactions are tuned using real results of the outlet temperatures and components in industrial operating conditions. At the next stage, validation of the model was carried out using a new naphtha feed in industrial scale. The final stage of this research was based on splitting a naphtha feed using its only ASTM boiling point and specific gravity, to converting to the components and applying into the process model to predict the outlet temperature and composition, the reformate yield and RON, hydrogen and LPG product, and coke formation at each cycle. The predicted and commercially reported results agreed with each other.

KEYWORDS: naphtha reforming, gasoline, high RON, continuous catalytic reformer

*Please send correspondence to Shohreh Fatemi, email: shfatemi@ut.ac.ir.

Introduction

The major refinery process for upgrading low-octane naphtha consisting of C_5 to C_{12} hydrocarbons to high-octane gasoline is catalytic reforming and also this process is a great interest to the petrochemical industry for the production of aromatic compounds that are raw materials for plastics, elastomers and resins manufacture. Hydrogen, light hydrocarbons and LPG are also obtained as side products. [1]

Generally the reforming process is carried out in three or four series adiabatic reactors with their interstage heaters. The temperature variation within the columns is 450 °C to 550 °C.

A variety of catalytic reforming processes are available which differ in the type and composition of the catalyst, the regeneration procedure (cyclic, semi-regenerative or continuous) or the configuration of the equipments [2-3]. Continuous catalytic reforming of naphtha is a new technology in recent years because of economic design, operability and product quality in comparison to the other types of catalytic reforming units. Today, all new units are designed based on this technology and old units are revamped to the continuous process or combination of both. There are some advantages of CCR (Continuous Catalytic Reforming) process against traditional methods such as; production of the higher octane reformate even working with a low feed quality, long time working of the process for hydrogen demand, using catalyst with less stability but higher selectivity and yield, the lower required recycle ratio and the lower operational pressure with high yield of hydrogen.

The kinetics of catalytic reforming has been attracting the attention of many researchers. The naphtha feed is very complex consisting of several hundred components and each of them undergoes various reactions. By this reason, it is common to assume that only three classes of hydrocarbons are present in naphtha (paraffins, naphthenes and aromatics), and they are considered to have similar properties and kinetic behavior. [4-9]

The purpose of this work is modeling and simulation of the CCR unit and evaluation of the results by comparison with an industrially designed process. De-lumping the naphtha feed from its ASTM distillation curve is performed in another part of the project in order to derive a more applicable model for simulation of industrial reformer units that there is not detailed information about the molecular feed composition.

Kinetic modeling of Reactions

An effective kinetic reforming must properly represent all the major types of reactions. The large number of reactions and hundreds of components taking part in the actual reaction system make this a rather complex problem.

To reduce the complexity of reactions, the large number of chemical components is assigned to smaller set of lump components. [4,5] In the present model, the naphtha feed has been characterized by 25 groups, ranging from six to ten carbon atoms for normal and isoparaffins (P_6 - P_{10}), from six to ten atoms of carbon for alkylcyclopentanes, alkylcyclohexans (N_6 - N_{10}) and aromatics (A_6 - A_{10}). Considering C_1 to C_5 hydrocarbons as the LPG product and hydrogen with those mentioned compounds, there would be 31 components which are regarded as the reactants and product ingredients.

There are 12 sets of kinetic reactions in present model such as dehydrogenation and dehydroisomerization of naphthenes to aromatics, dehydrogenation of paraffins, dehydrocyclization of paraffins to aromatics, isomerization or hydroisomerization to isoparaffins, isomerization of alkylcyclopentanes, and substituted aromatics and hydrocracking of paraffins and naphthenes to lower hydrocarbons. The reactions and their kinetic rates are presented in Table 1.[4]

The internal and external mass transfer resistances are ignored in the mole balance and energy balance equations because of the previous investigations found in the literatures. Ressev and Stoica studied the effect of external mass transfer resistance and they found that this effect can be ignored when the Reynold's number is more than four, as there exists in the industrial reactors. Naturally, the effect of internal diffusion may be decreased or even completely eliminated by using a more porous structure for alumina support. This explains the evolution of industrial catalysts from having a total pore volume of 0.48 cm³/g catalyst in 1975–1978 to a value of 0.6–0.7 cm³/g catalyst at the present time.

In contrast to the cyclic reforming process, the continuous catalytic reformers (CCR) are operated at lower pressures (up to 0.5 Mpa), therefore coking and deactivation of the catalyst is unavoidable, and continuous regeneration of the catalyst should be performed in the moving bed reactors. Many researches are implemented for modeling of catalyst deactivation by coke formation and activity variation of the reforming catalyst [3,7]. At the present work, activity coefficient of the catalyst has been taken as a function of residence time, in the reactor. The activity function and coke formation are introduced by the following relations. [10,11]

$$r_i = r_i^0 \phi_i \quad , \quad 0 \leq \phi_i \leq 1$$

$$\phi_i = e^{-\alpha_i C_c}$$

$$\frac{dC}{dw} = \frac{r_{c_0}}{u_s} \exp(-\alpha C)$$

$$r_{c_0} = k_2 \frac{P_{ACP}}{P_{H_2}^2}$$

$$k_2 = Ae^{-E/RT}$$

Table 1. The considered reactions and rate equations in reforming process.[4]

Dehydrogenation	$ACH_n \longleftrightarrow A_n + 3H_2; \quad \frac{dF_1}{dw} = k_{1n} \left(P_{ACH_n} - \frac{P_{A_n} P_{H_2}^3}{K_{1n}} \right) = r_{1n}$
Ring Expansion	$ACH_n + H_2 \longleftrightarrow NP_n; \quad \frac{dF_3}{dw} = k_{3n} \left(P_{ACH_n} P_{H_2} - \frac{P_{NP_n}}{K_{3n}} \right) = r_{3n}$
	$ACH_n + H_2 \longleftrightarrow IP_n; \quad \frac{dF_4}{dw} = k_{4n} \left(P_{ACH_n} P_{H_2} - \frac{P_{IP_n}}{K_{4n}} \right) = r_{4n}$
	$NP_n \longleftrightarrow ACP_n + H_2; \quad \frac{dF_5}{dw} = k_{5n} \left(P_{NP_n} - \frac{P_{ACP_n} P_{H_2}}{K_{5n}} \right) = r_{5n}$
	$IP_n \longleftrightarrow ACP_n + H_2; \quad \frac{dF_6}{dw} = k_{6n} \left(P_{IP_n} - \frac{P_{ACP_n} P_{H_2}}{K_{6n}} \right) = r_{6n}$
Isomerization	$NP_n \longleftrightarrow IP_n; \quad \frac{dF_7}{dw} = k_{7n} \left(P_{NP_n} - \frac{P_{IP_n}}{K_{7n}} \right) = r_{7n}$
	$ACP_n \longleftrightarrow ACH_n; \quad \frac{dF_2}{dw} = k_{2n} \left(P_{ACP_n} - \frac{P_{ACH_n}}{K_{2n}} \right) = r_{2n}$
Hydrocracking	$NP_n + \frac{n-3}{3} H_2 \longleftrightarrow \frac{n}{15} \sum_{i=1}^5 C_i; \quad \frac{dF_8}{dw} = k_{8n} \left(\frac{P_{NP_n}}{P_t} \right) = r_{8n}$
	$IP_n + \frac{n-3}{3} H_2 \longleftrightarrow \frac{n}{15} \sum_{i=1}^5 C_i; \quad \frac{dF_9}{dw} = k_{9n} \left(\frac{P_{IP_n}}{P_t} \right) = r_{9n}$
	$ACH_n + \frac{n}{3} H_2 \longleftrightarrow \frac{n}{15} \sum_{i=1}^5 C_i; \quad \frac{dF_{10}}{dw} = k_{10n} \left(\frac{P_{ACH_n}}{P_t} \right) = r_{10n}$
	$ACP_n + \frac{n}{3} H_2 \longleftrightarrow \frac{n}{15} \sum_{i=1}^5 C_i; \quad \frac{dF_{11}}{dw} = k_{11n} \left(\frac{P_{ACP_n}}{P_t} \right) = r_{11n}$
Hydrodealkylation	$A_{n+1} + H_2 \longleftrightarrow A_n + CH_4; \quad \frac{dF_{12}}{dw} = k_{12n} P_{A_{n+1}} P_{H_2}^{0.5} = r_{12n}$

Mass and energy balance equations

Mole balance equation of each specie is written as following;

$$\frac{dF_i}{dw} = \sum_{j=1}^{56} r_j (StCo)_{j,i} \quad ; i = 1 \text{ to } 30$$

Energy balance should be provided for each reactor as follows;

$$\frac{dT}{dw} = \frac{\sum_{n=6}^{10} \left(\sum_{i=1}^{12} (-\Delta H_{in}) r_{in} \right)}{\sum F_j C_{p_j}}$$

Total Pressure is another function which should be accounted in the model. Pressure drop is predicted by Ergun's equation. The coefficients of the equation are modified to be used in moving bed type reactors [3].

$$\frac{dP}{dw} = - \left(\alpha G + \frac{\beta \mu_g (1 - \varepsilon)}{D_p} \right) \frac{G}{\rho_g D_p \varepsilon^3}$$

Also because of the radial flow pattern in the reactors, mass flux of the gas (G) was related to the mass of the catalyst (w) as the following:

$$G = \frac{m}{A_c}$$

$$\frac{dA_c}{dw} = - \frac{2\pi L}{A_c \rho_c (1 - \varepsilon)}$$

The model integrates numerically the mass, energy and pressure drop differential equations by forth order Runge-Kutta method for each individual reactor.

Prediction and tuning of the reactions' pre-exponential terms and activation energies were performed by comparison the outlet results of each reactor with experimental data. An objective function was introduced as the following form to be minimized. The optimization process was carried out by Nelder-Mead method. The flowchart of tuning the parameters is shown in Fig. 1

$$\psi = \sum_{i=1}^{31} (F_i^{Model} - F_i^{Exp.})^2 + \sum_{i=1}^3 (T_i^{Model} - T_i^{Exp.})^2$$

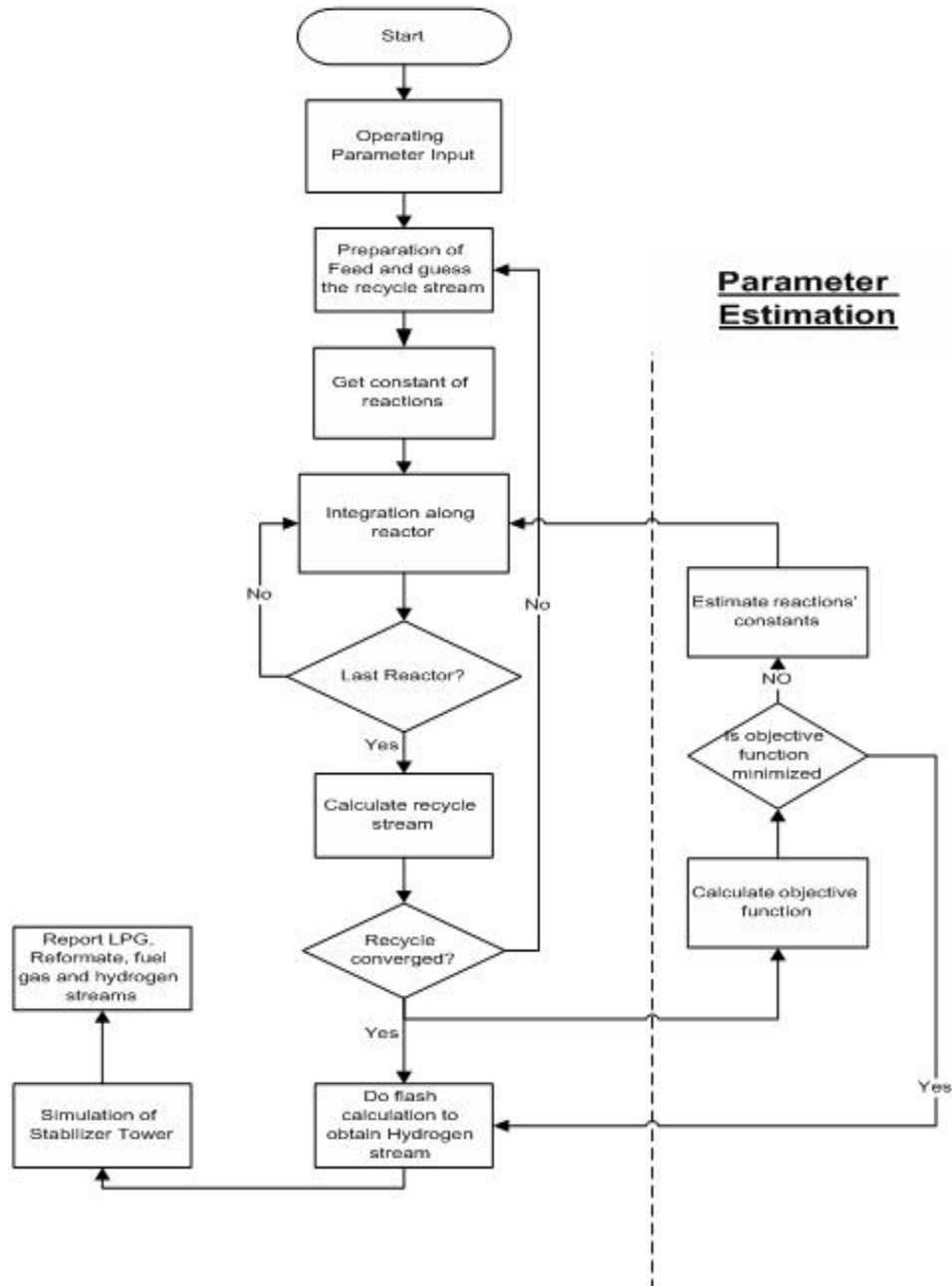


Figure 1: The flowchart of the kinetic parameters optimization

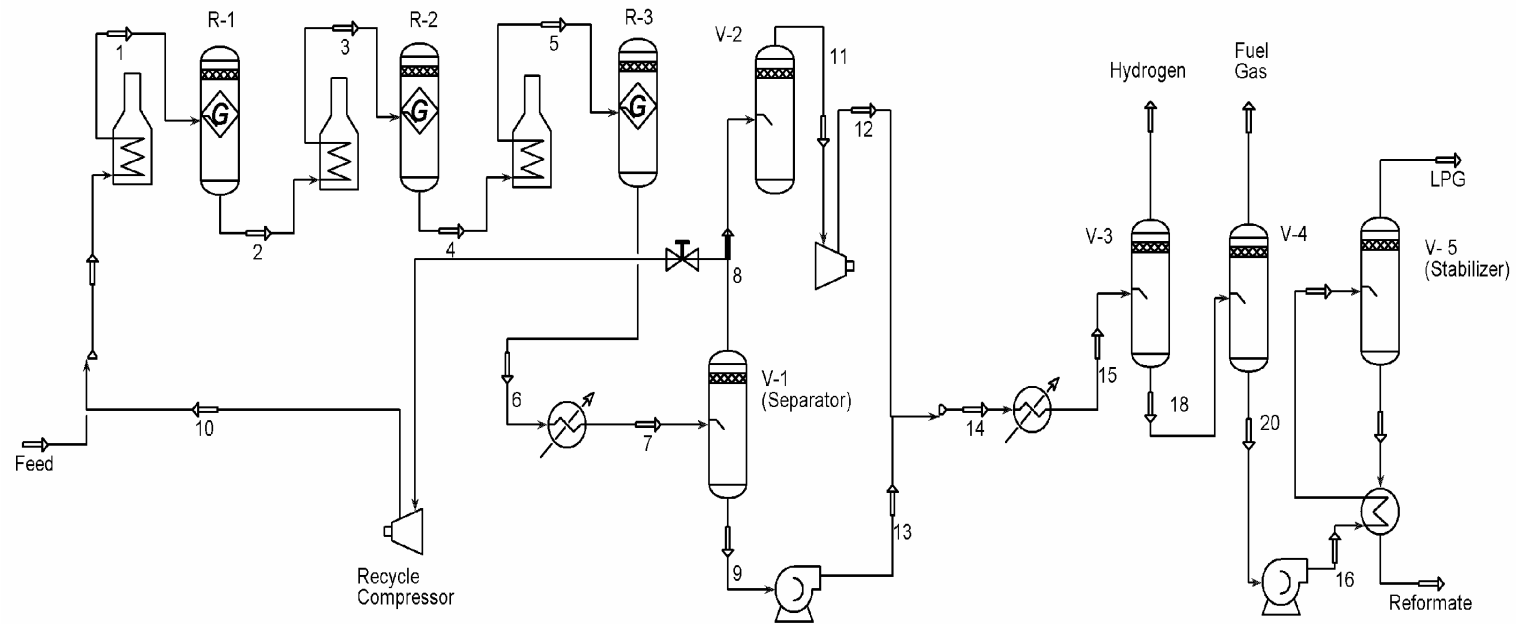
Commercial Process Specification

Following is a brief process description of commercial unit as shown in Fig. 2. Feed to the Catalytic Reforming unit, hydrotreated heavy Naphtha, mixed with the recycle hydrogen from the recycle compressor and heated to the required first reactor inlet temperature. The reactors are radial flow types, the feed flowing through the catalyst bed from the outer circumference towards the center pipe. In the first reactor, the reactions are predominantly endothermic and therefore the reactor effluent requires reheating in the first interheater to the required inlet temperature of the second reactor. The reactions in this reactor are less endothermic but still require reheating in before entering the third reactor. The inlet temperatures of the three reactors are identical. These inlet temperatures are gradually increased through the catalyst life time.

In the three reactors, the feed is contacted with the reforming catalyst. The catalyst circulates continuously from one reactor bottom to the top of the next one and then to the regeneration section and return to the first reactor. The effluent is cooled before entering the separator drum. A portion of the separated gas is compressed in recycle gas compressor and is recycled to the reactors. The remaining gas which constitutes the hydrogen production gas is routed to a compressor and recontact with separated liquid. The recontacted mixture is then cooled, and hydrogen is separated from liquid. The separated liquid then flashed to obtain light ends i.e. C_1 and C_2 's (Fuel gas), and remained liquid is pumped to enter the stabilizer column. The stabilizer overhead is LPG. Reformate from the bottom of the stabilizer is cooled in the stabilizer feed/bottom exchanger and sent to the storage. The operational conditions and catalyst properties are shown in Table 2 and 3, respectively.

Table 2. Process Specification of CCR unit

No. of Reactors	3
Feed WHSV	2.5 kg/kg/hr
Inlet Pressure	0.54 MPa
Hydrogen Recycle ratio	1.56 (H ₂ /HC)
Inlet Temperatures	519 C
Catalyst fractions	20/30/50
Total catalyst weight	54800 Kg
Catalyst flow rate	744 Kg/hr



V-1 (Separator)		V-3		V-5 (Stabilizer)		R-2	
Vessel Temperature	39.00 C	Vessel Temperature	38.00 C	Vessel Temperature	39/260 C	Vessel Temperature	522.0 C
Vessel Pressure	3.300 bar	Vessel Pressure	28.00 bar	Vessel Pressure	16.5/18 bar	Vessel Pressure	5.000 bar

V-2		V-4		R-1		R-3	
Vessel Temperature	39.00 C	Vessel Temperature	41.00 C	Vessel Temperature	522.0 C	Vessel Temperature	522.0 C
Vessel Pressure	3.300 bar	Vessel Pressure	16.00 bar	Vessel Pressure	5.400 bar	Vessel Pressure	4.500 bar

Figure 2. Schematic of commercial CCR unit and operating conditions

Table 3. Catalyst characterization

Kind of Catalyst	Pt-Sn/Al ₂ O ₃
Size and shape	Spherical-1.8 mm diameter
Particle density	690 kg/m ³
Particle porosity	0.6

Feed characterization

The analysis of the naphtha feed is usually reported in terms of its ASTM distillation curve and API gravity. Since the kinetic model is based on lumped pseudo-components, therefore feed characterization technique was implemented to infer the composition of the lumped components. The model used in this study is based on Albahri model.

This model is based on the concept that the global properties of petroleum fraction must be equal to those calculated from the pure components contained in that fraction. When both bulk and pure component properties are available, the composition of the petroleum fraction may be simulated using optimization algorithm. It has been shown that the average physical properties of the petroleum fraction can be calculated by integration of the pure component properties along the true boiling point curve according to the following relation.

$$\theta = \int_0^1 \theta(x) dx$$

Where x is the fraction of volume vaporized in TBP distillation, $\theta(x)$ is the property value at x. For a finite number of components, the equation is changed to:

$$\theta = \sum_{i=1}^n \theta_i(x) \Delta x_i$$

In selection of physical properties it should be noted that some properties are not defined for light component in naphtha such as pour point, cloud point, etc., therefore in our study, the following properties were defined; Critical properties, molecular weight, refractive index, Watson characterization factor,

heat capacity, surface tension, viscosity and standard density. Mixing rule for Watson characterization factor and heat capacity are based on mass fraction, while molar volume is defined on volumetric fraction and the others are introduced on the base of mole fractions.

Following objective function should be minimized to estimate the composition related to proposed ASTM curve.

$$\psi = \sum_{i=1}^n \frac{|Tb_i - Tb'_i|}{Tb_i} \times 100 + \sum_{j=1}^m \frac{|\theta_j - \theta'_j|}{\theta_j} \times 100$$

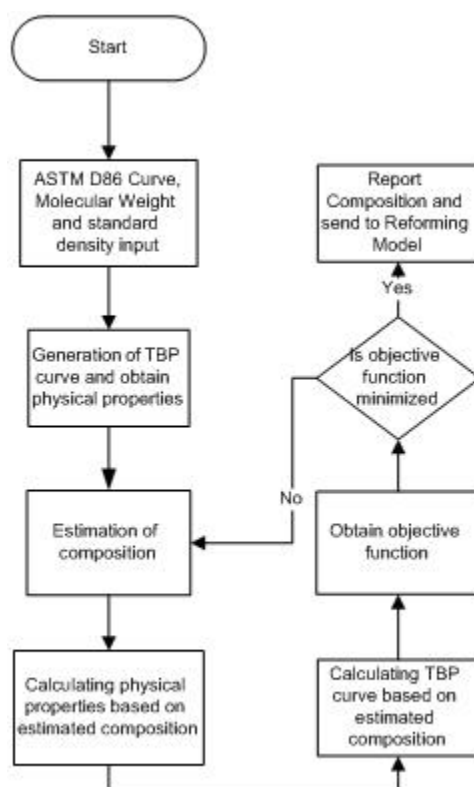


Figure 3. Flowchart of Feed Characterization program

In Table 4, comparison of calculated values from ASTM curve and estimated composition is presented.

Fig. 4 shows experimental ASTM D-86 curve for Feed and estimated curve based on feed characterized components.

Table 4. Comparison of physical properties of feed, calculated values from ASTM curve (1) and estimated composition (2)

Physical property	unit	1	2
Critical Temperature	K	589.05	588.17
Critical Pressure	bar	28.17	28.29
Critical Volume	m ³ /kgmol	0.45	0.46
Acentricity		0.34	0.37
Refractive Index		1.42	1.43
Molecular Weight		116.01	116.01
Watson characterization factor		11.91	11.88
Heat Capacity @ 25 °C	kJ/kg°C	1.94	1.96
Surface Tension @ 25 °C	dyne/cm	23.12	23.43
Viscosity @ 37 °C	cP	0.52	0.54
Molar Volume	m ³ /kgmol	0.15	0.15
Heat Conductivity	W/m°C	0.13	0.13
Critical Temperature	K	589.05	588.17
1 : Calculated from experimental ASTM curve			
2 : Calculated from estimated composition			

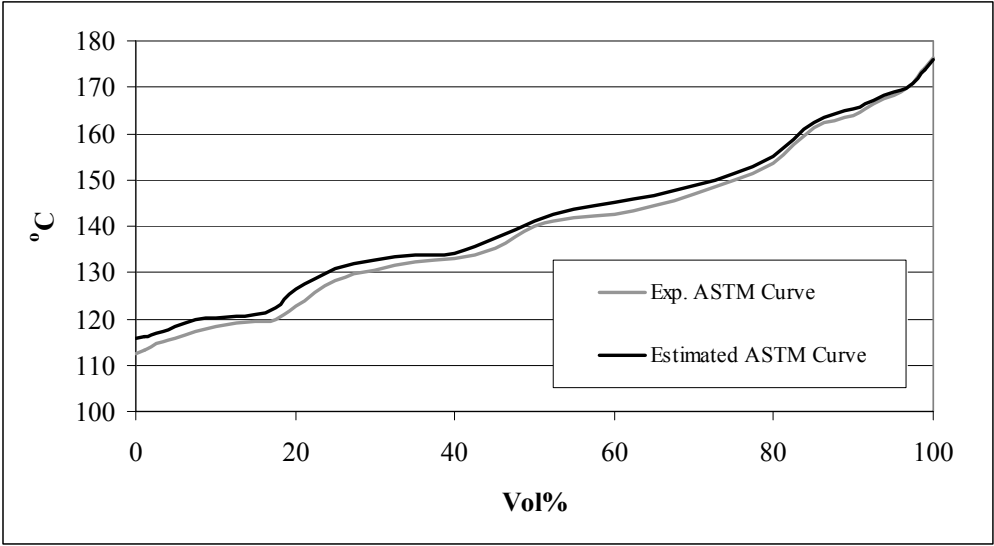


Figure 4. Estimated and Experimental ASTM-D86 Curve for Feed

Table 5. Predicted feed composition from ASTM boiling point (Mol%)

Comp.	Predicted	Comp.	Predicted
5N6	0.02	nP9	9.37
5N7	5.70	nP10	5.99
5N8	2.43	iP6	0.00
5N9	1.13	iP7	2.71
5N10	0.00	iP8	4.68
6N6	0.04	iP9	9.66
6N7	3.13	iP10	5.17
6N8	10.33	A6	0.03
6N9	3.29	A7	4.77
6N10	3.00	A8	6.04
nP6	0.01	A9	5.18
nP7	8.82	A10	1.15
nP8	7.34		

Results and Discussion

The molar flow variation of the components, temperatures and coke formation are derived by the model simulation and reported in Figs. 5 to 8. Also the actual outlet results exhibited in the figures are in a good agreement with the model.

As seen in Fig. 5, Naphthenes concentration is decreased along the reactions especially in the first reactor. Dehydrogenation reaction is endothermic reaction therefore by decreasing the Naphthenes' concentration, temperature is more reduced in the first reactor than the others as seen in Fig. 6. Also, Cyclization reaction of the paraffins which is an endothermic reaction causes temperature reduction, although this effect appears in the second and third reactors instead of the first one because of its lower rate than the dehydrogenation. In the two last reactors, temperature is high enough and hydrogen is present to perform the hydrocracking reactions which enhance production of light ends, as can be seen in Fig. 5. As observed in Fig. 7, the coke formation is growing up faster in the first reactor than the last one because of the more rapidly dehydrogenation reaction on the catalyst metal sites in the first reactor. In the last

reactor, although hydrocaracking is occurred faster on the acid sites, lower rate of coke formation is observed because of presence of enough hydrogen.

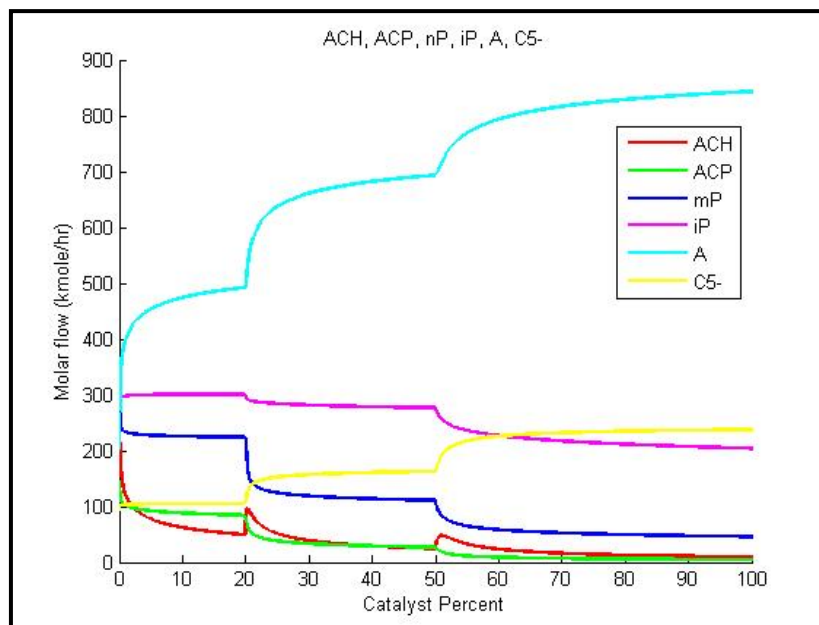


Fig.(5). Molar flow of the lump components derived by the model

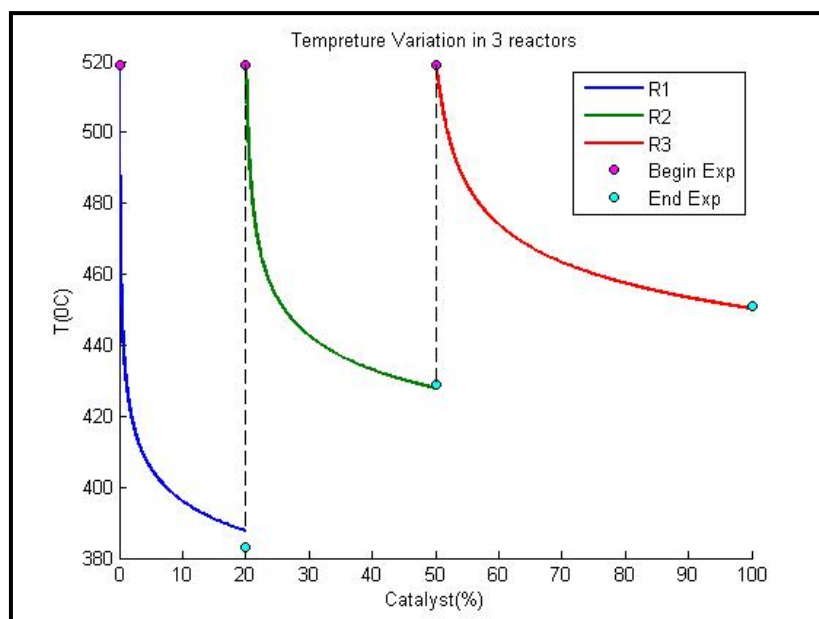


Fig.(6). Temperature profiles and comparison with the outlet results

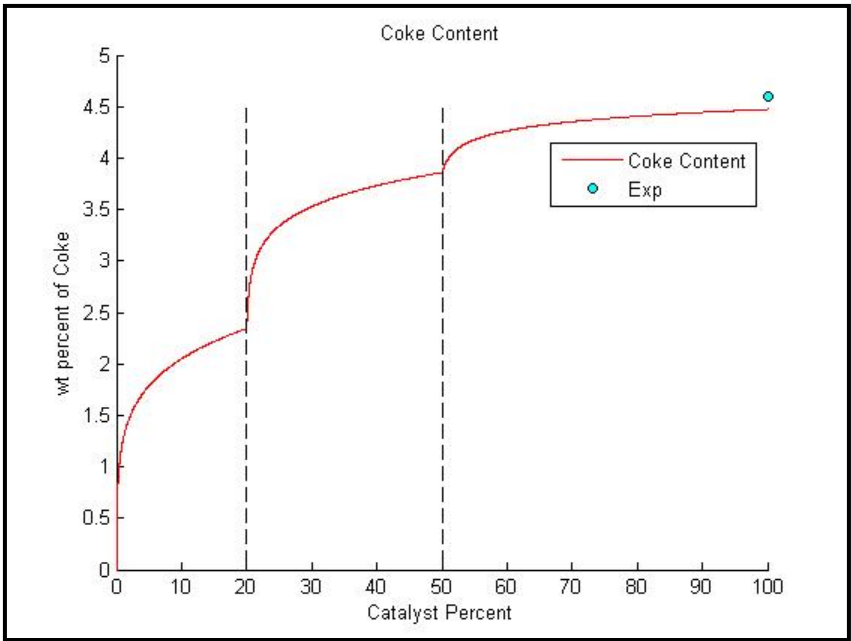


Fig.(7) Coke formation profile and comparison with the end part.

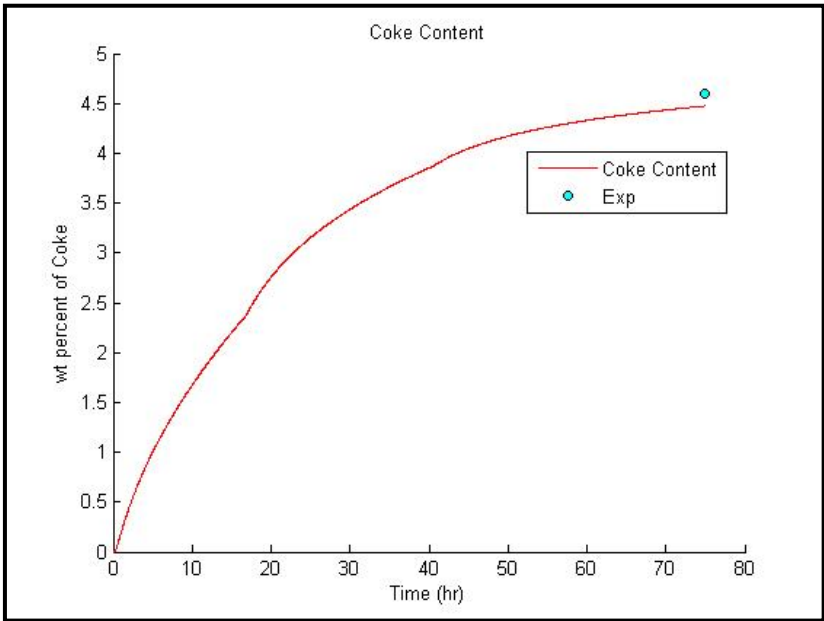


Fig.(8) Coke formation along the Cycle time and comparison with the end part.

Pressure drop profiles and superficial velocity of the fluid are shown in Figs 9 and 10 as the function of reactors' radius. Avoiding the pressure drop of reaction section is important whereas decreasing the size of catalyst particles, for elimination internal diffusion effects, causes pressure drop enhancement the flow pattern of the feed is designed to distribute radially through the reactors. In this situation, fluid velocity should be such that cavity and pinning effects does not occur in the catalyst bed. As indicated in Fig 9, pressure drop profile of each reactor along the reactor radius is obtained low enough and the cost of compression and operating pressure in continuous catalytic reforming process would be economical.

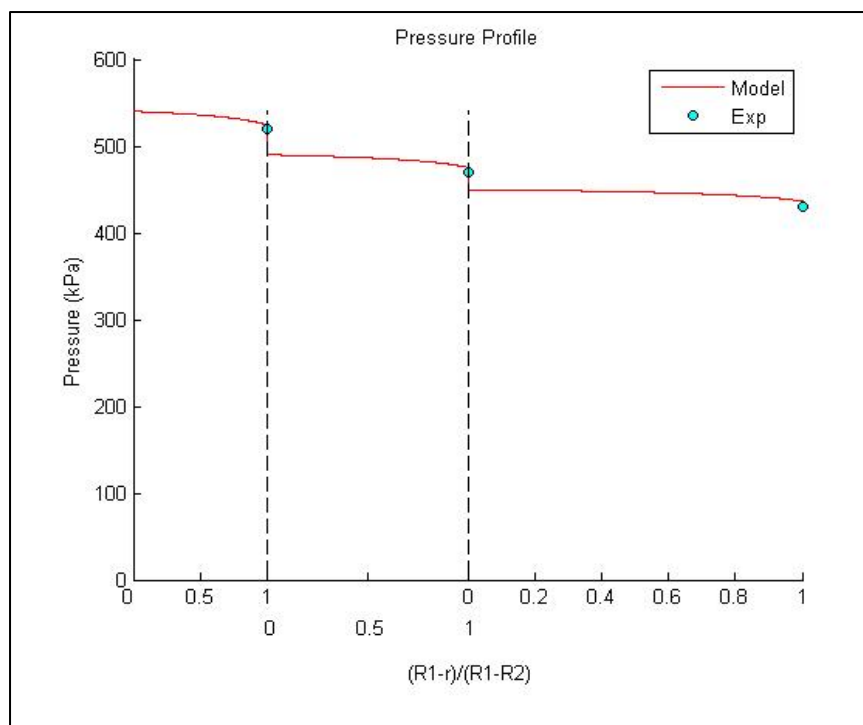


Fig.(9) Pressure drop of the reactors versus nondimensional radius and comparison to the end part.

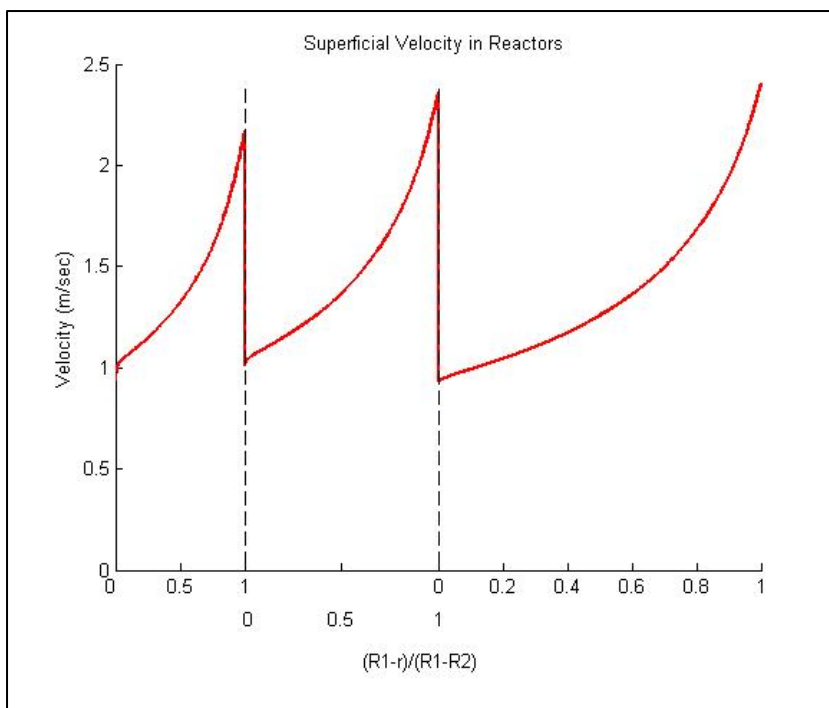


Fig.(10). Superficial velocity of the fluid in the reactors, versus nondimensional reactor radius

After optimization of kinetic parameters to approach to the actual results, the extended model was validated by replacing the feed specification by a new naphtha feed stream (No.2). The results showed a good agreement between predicted and commercially reported amounts with average relative deviation of 4%. A comparison between the model and actual results are presented by the average absolute relative deviation (AARD) in Table 6.

Conclusion

A process model for continuous catalytic naphtha reforming has been developed. This model is used for simulating a commercial continuous unit consisting of a series of three catalytic reforming reactors.

The process model includes a kinetic model which takes into account the most important reactions of the catalytic reforming process in terms of isomers of the same nature. Reformate composition and temperature profiles have been obtained to provide information about the conversion, flow rate, yield, pressure drop, fluid velocity, coke formation and catalyst decay in each of the reactors.

The presented package can admit a lumped feed with ASTM distillation and recognize the fractions using physical properties and delump the feed to various hydrocarbon groups, thereafter the reforming process can be performed by the numerical package and report the temperature, product composition and its properties such as RON, ASTM BP, reformate, LPG and hydrogen yield.

Table (6). AARD% of the outlet properties by the model using two different feeds.

3rd Reactor Outlet Yield (wt %)		
	Feed1	Feed2
C5+	0.01	0.24
Tol	0.92	3.70
A8	0.91	2.00
A9	1.21	2.84
A10+	0.61	5.65
H2	0.82	3.00
C5-	1.61	5.72
Hydrogen		
	Feed1	Feed2
H2 (mol %)	0.12	0.20
Flowrate	1.75	4.88
Reformate		
	Feed1	Feed2
RON	0.70	1.00
MON	0.89	1.68
Aromatic (Vol%) (ASTM D86)	1.77	3.56
IBP	15.61	24.04
10%	0.78	0.96
50%	0.42	0.21
90%	0.00	0.64
EP	0.16	0.00
Flowrate	0.39	0.23
Temperature		
	Feed1	Feed2
1st Reactor	0.73	0.99
2nd Reactor	0.13	0.56
3rd Reactor	0.07	0.30

References

- [1] Antos G., Aitani A.M., Parera J.M., “*Catalytic Naphtha Reforming Science and Technology*”, , Marcel Dekker Inc., 1995.
- [2] J. Ancheyta-Jua’ rez,, E. Villafuerte-Macý’as, L. Dý’az-Garcý’a, and E. Gonza’lez-Arredondo,"Modeling and Simulation of Four Catalytic Reactors in Series for Naphtha Reforming", *Energy & Fuels* 2001, 15, 887-893.
- [3] J. W. Lee, Y. C. Ko, Y. K. Jung and K. S. Lee, E. S. Yoon, "A modeling and simulation study on a naphtha reforming unit with a catalyst circulation and regeneration system", *Computers & Chemical Engineering* ,Vol. 21, 20 May, 1997, S1105-S1110.
- [4] Padmavathi G., Chaudhuri K. K., “*Modeling and Simulation of Commercial Catalytic Naphtha Reformers*”, *The Canadian Journal of Chem. Eng.*, 75, 930-937(1997).
- [5] Jorge Ancheyta-Jua’ rez* and Eduardo Villafuerte-Macý’as,"Kinetic Modeling of Naphtha Catalytic Reforming Reactions",*Energy & Fuels* 2000, 14, 1032-1037.
- [6] Marin G.B., Froment G.F., “*Reforming of C6 Hydrocarbons on A Pt-Al2O3 Catalyst*”, *Chem. Eng. Sci.*, 37, 759-773(1982).
- [7] Rahimpour M.R., Esmaili S., Bagheri N., “*A Kinetic and Deactivation Model for Industrial Catalytic Naphtha Reforming*”, *Iranian Journal of Sci. & Tech. B*, 27, 281-290(2003)
- [8] Shanying H., Zhu F., “*Molecular Modeling and Optimization for Catalytic Reforming*”, *Chem. Eng. Comm.*, 191, 500-512(2004).
- [9] J. Ancheyta, E. Villafuerte, P. Schachat, R. Aguilar, E. Gonzalez, “Simulation of a Commercial Semiregenerative Reforming Plant Using Feedstocks with and without Benzene Precursors,” *Chem. Eng. Technol.* 25, 5. (2002).
- [10] Liu K., Fung S.C., and D.S. Rumschitzki,”Kinetics of Catalyst Coking in Heptane Reforming Over Pt-Re/Al2O3”,*I.E.C.Res.*, 36(8),(1997)3264.
- [11] Liu K., Fung S.C., and D.S. Rumschitzki,”Heptane Reforming Over Pt-Re/Al2O3 , Reaction Network” *J. Cat.*, 206(2), (2002)188.